Military Technical College
Kobry El-Kobbah,
Cairo, Egypt

9th International Conference
on Electrical Engineering
ICEENG 2014

Improving Power Flow of Power Transmission System Using UPFC

By

Heba Allah R. Ahmed* T. S. Abdel Salam* M. A. Mostafa * M. A. L. Badr*

Abstract:

This paper introduces the mathematical modeling of an advanced member of flexible ac transmission systems (FACTS) controller which is a unified power flow controller (UPFC). This model submitted the implementation of the device in conventional Newton–Raphson (NR) power flow algorithm; it is derived from two-voltage source represented and analyzed in detail. The model takes operational losses of UPFC into account so it represents a more robust and feasible alternative than other methods. Based on the proposed model a program in Matlab language has been written to extend conventional NR algorithm. A computer simulation study performed on IEEE 14-bus test system and IEEE 30-bus test system are presented to test the approach by locating the UPFC anywhere in a power system. The effect of UPFC allocation on power system operation has been investigated in detail and the power losses minimization of the power system with UPFC has been achieved using the proposed method by adjusting the location of UPFC with a proper adjustment of UPFC parameters.

Keywords:
FACTS, flexible AC transmission systems, MATLAB, Newton-Raphson load flow, power flow and Unified Power Flow Controller (UPFC)

* Faculty of Engineering, Ain-Shams University, Cairo-Egypt.

1. Introduction:

The possibility of controlling power flow in an electric power system without generation rescheduling in order to improve the power system performance is not an easy process; however the fast development of power electronics technology has introduced the FACTS as a promising concept for power system applications during the last decade [1].
By the use of FACTS technology, power flow along the transmission lines can be more secured, reliable and flexibly controlled. UPFC is one of the more interesting members of FACTS controller devices which have the capability to control all the three transmission parameters (voltage, impedance and phase angle).

The performance of the UPFC for power flow control by deriving a mathematical modeling of unified power flow controller (UPFC) will be investigated and the implementation of the device in conventional Newton–Raphson (NR) power flow algorithm is proposed by this model. The model is derived from two-voltage source represented and analyzed in detail. It is considered to be more robust than others as it takes operational losses of UPFC into account. A program in Matlab language is written by extending conventional NR algorithm based on proposed model.

This paper is organized as follows: part 2 describes the construction and operating principle of UPFC. Part 3 explains the basic control functions of UPFC. Part 4 develops a steady state model for UPFC. Part 5 discusses the implementation of the model for power flow studies. Part 6 demonstrates the application of UPFC in optimal power flow control through numerical examples for different case studies. Part 7 gives the overall conclusions of the research work.

2. Construction and Operation of UPFC:

UPFC as shown in Fig.1. consists of two switching converters. These converters are operated from a shunt transformer and linked by common dc link provided by a dc storage capacitor [2]. Converter 2 injects an ac voltage V_{ser} with controllable magnitude Vser ($0 \leq V_{ser} \leq V_{sermax}$) and phase angle θ_{ser} ($0 \leq \theta_{ser} \leq 360$) which provides the main function of the UPFC. The voltage is injected in series with the line via an insertion transformer. The injected voltage is considered to be a synchronous voltage source. The transmission line current flows through this voltage source which causes real and reactive power to be exchanged between it and the ac system. The real power converted by the first converter into dc power exchanged at the ac terminal appeared at the dc link

as positive or negative real power demand, while the reactive power exchanged at the ac terminal is generated internally by the first converter [3-5].
The basic function of converter 1 is supplying or absorbing the real power needed by converter 2 at the common dc link. This dc link power is converted back to ac and connected to the transmission line by a series-connected transformer. Converter 1 also generates or absorbs controllable reactive power and it can provide independent shunt reactive compensation for the line [3].
It is significant to note that there is a closed path for the real power negotiated by the action of series voltage injection through converters 1 and 2 back to the line, the corresponding reactive power exchanged is supplied or absorbed locally by converter 2 and therefore it does not flow through the line. Thus, converter 1 can be operated at a unity power factor or controlled to have a reactive power exchange with the line independently of the reactive power exchanged by the converter 2. This means that there is no continuous reactive power flow through UPFC [3], [6].

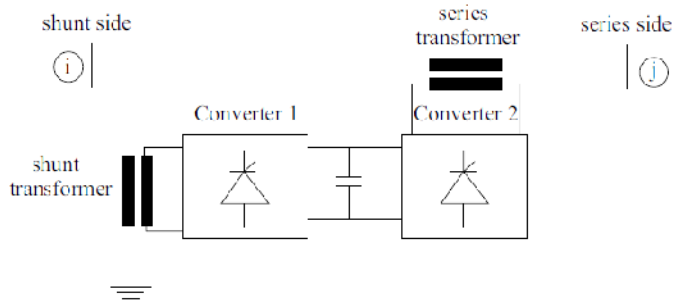

Figure (1): *Basic circuit arrangement of UPFC [3]*

3. Basic Control Functions:

With this operational flexibility, UPFC might be used for the purposes of terminal voltage regulation, series compensation, and transmission angle regulation. Fig.2. describes the phasor relationships of these operating modes. Terminal voltage regulation is similar to that attainable with a transformer tap-changer having infinitely small steps is shown in Fig.2.(a). The series voltage Vser is injected either in-phase or out-phase with sending end voltage Vs. Namely Vser= ±DVo. Series reactive compensation is shown schematically in Fig.2.(b). The series voltage Vser is injected either 90˚ lagging or 90˚ leading with the transmission line current I_L. In this case Vser= ±Vc. The phase shifting is shown schematically in Fig.2. (c). The series voltage Vser is injected with an angular relationship with respect to Vs so that the desired σ phase shift (leading or lagging) without any change in magnitude is achieved. In this mode Vser= ±Vσ. In multi-function control mode, the injected series voltage Vser is controlled to meet

simultaneous terminal voltage regulation, series compensation, and phase shifting. In this multi-function mode, Vser = DVo + Vc + Vσ. The resulting voltage phasors is observed in Fig.2.(d) [3],[7-8].

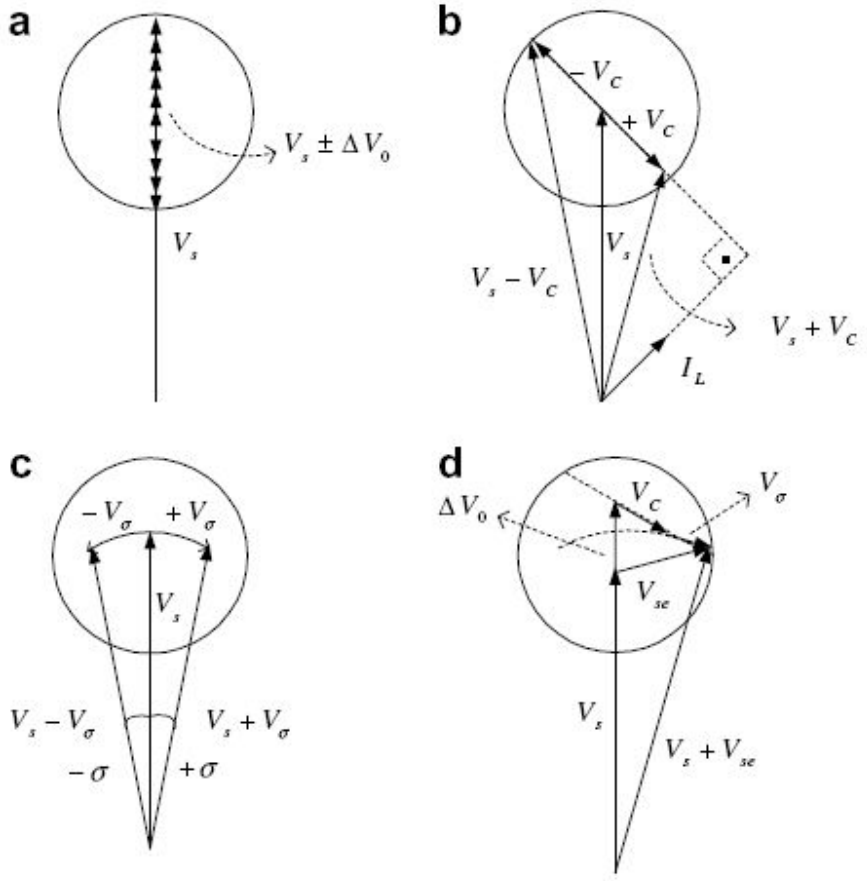

Figure (2): *Basic UPFC control functions: (a) terminal voltage regulation, (b) Series reactive compensation, (c) phase angle regulation, and (d) Multifunction power control mode.*

4. Modeling of UPFC [7],[9-10]:

A UPFC is represented in the steady-state conditions as shown in Fig.3. by two voltage sources representing fundamental components of output voltage waveforms of the two converters and impedances being the leakage reactances of the two coupling transformers. The voltage sources, V_{ser} and $V_{sh,}$ are controllable in both magnitudes and phase angles.

V_{ser} can be assumed to be:

$$V_{ser} = rV_i e^{j\theta_{ser}} \quad (1)$$

The values of r and θ_{ser} are defined within specified limits. The variable r represent certain percent of the voltage magnitude V_i at bus i.

$$0 \le r \le r_{max} \text{ and } 0 \le \theta_{ser} \le 2\pi. \quad (2)$$

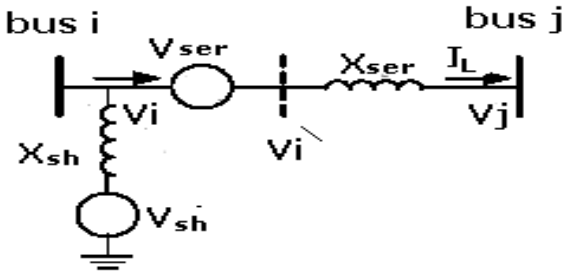

Figure (3): *UPFC equivalent circuit*

4.1. Series Connected Voltage Source Converter Model:

The steady-state UPFC mathematical injection model is developed by replacing voltage source V_{ser} by a current source I_{ser} parallel with a susceptance $b_{ser} = 1/X_{ser}$. Therefore, the series current I_{ser} is defined by:

$$I_{ser} = -jb_{ser}V_{ser} \quad (3)$$

The current source I_{ser} can be modeled by injected power at the two buses i and j between which the UPFC is connected as shown in Fig.4.

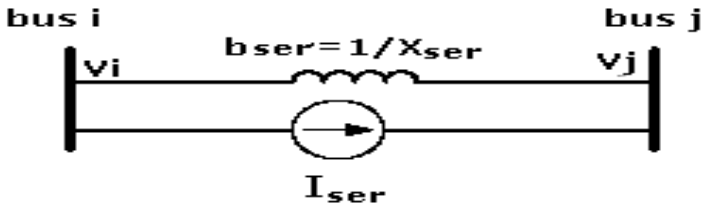

Figure (4): *Replacement of series voltage source by a current source*

$$S_{iser} = V_i(-I_{ser})^* \quad (4)$$

$$S_{jser} = V_j(I_{ser})^* \quad (5)$$

The injected powers S_{iser} and S_{jser} can be simplified according to the following operations, by substituting equations (1) and (3) into (4) and (5). The power injected at bus i is found by substituting equations (1)and (3) into (4) to yield:

$$S_{iser} = V_i(jb_{ser}rV_i e^{j\theta_{ser}})^* \quad (6)$$

By using the Euler Identity, ($e^{j\theta_{ser}} = \cos\theta_{ser} + j\sin\theta_{ser}$), equation (3-16) takes the form:

$$S_{iser} = V_i (e^{-j(\theta_{ser}+90)} b_{ser} r V_i^{*}) \quad (7)$$

$$S_{iser} = V_i^{2} b_{ser} r \left[\cos(-\theta_{ser} - 90) + j\sin(-\theta_{ser} - 90)\right]. \quad (8)$$

By using trigonometric identities, equation (8) reduces to:

$$S_{is} = -r b_{ser} V_i^{2} \sin\theta_{ser} - j r b_{ser} V_i^{2} \cos\theta_{ser} \quad (9)$$

Equation (3-19) can be decomposed into its real and imaginary components,

$S_{iser} = P_{iser} + jQ_{iser}$, where

$$P_{iser} = -r b_{ser} V_i^{2} \sin\theta_{ser} \quad (10)$$

$$Q_{iser} = -r b_{ser} V_i^{2} \cos\theta_{ser} \quad (11)$$

Similarly the power injected at bus j is obtained by substituting equations (1) and (3) into (15) to yield:

$$S_{jser} = V_i V_j b_{ser} r \sin(\delta_i - \delta_j + \theta_{ser}) + j V_i V_j b_{ser} r \cos(\delta_i - \delta_j - \theta_{ser}) \quad (12)$$

Equation (12) can also be decomposed into its real and imaginary parts,

$S_{jser} = P_{jser} + jQ_{jser}$, with:

$$P_{jser} = V_i V_j b_{ser} r \sin(\delta_i - \delta_j - \theta_{ser}) \quad (13)$$

$$Q_{jser} = V_i V_j b_{ser} r \cos(\delta_i - \delta_j - \theta_{ser}) \quad (14)$$

Based on equations (10), (11), (13), and (14), the power injection model of the series connected voltage source can be seen as two dependent power injections at auxiliary buses i and j, as shown in Fig.5.

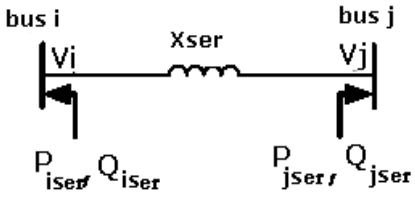

Figure (5): *Equivalent power injections of series branch*

4.2. Shunt Connected Voltage Source Converter Model:

In UPFC, the shunt branch is used mainly to provide both the real power, P_{ser}, which is injected to the system through the series branch, and the total losses within the UPFC. If the losses are to be neglected in the real power injection of the shunt connected voltage source at bus i, P_{sh} is equal to the injected series real power P_{ser} through the series connected voltage source to the system. This can be expressed by:

$$P_{ser} + P_{sh} = 0 \tag{15}$$

The apparent power supplied by the series converter is calculated as.

$$S_{ser} = V_{ser}I_{ij}^{*} = re^{j\theta_{ser}}V_i\left(\frac{V_i^{\backslash} - V_j}{jX_{ser}}\right)^{*} \tag{16}$$

Active and reactive power supplied by the series converter can be calculated from equation (16) as follows:

$$S_{ser} = re^{j\theta_{ser}}V_i\left(\left(re^{j\theta_{ser}}V_i + V_i - V_j\right)/jX_{ser}\right)^{*} \tag{17}$$

$$S_{ser} = rV_ie^{j(\delta_i+\theta_{ser})}\left(\left(rV_ie^{-j(\delta_i+\theta_{ser})} + V_ie^{-j\delta_i} - V_je^{-j\delta_j}\right)/-jX_{ser}\right) \tag{18}$$

$$S_{ser} = jb_{ser}r^2V_i^2 + jb_{ser}rV_i^2e^{j\theta_{ser}} - jb_{ser}rV_iV_je^{j(\delta_i-\delta_j+\theta_{ser})} \tag{19}$$

$$S_{ser} = jb_{ser}r^2V_i^2 + jb_{ser}rV_i^2(\cos\theta_{ser} + j\sin\theta_{ser}) - jb_{ser}rV_iV_j(\cos(\delta_i - \delta_j + \theta_{ser}) + j\sin(\delta_i - \delta_j + \theta_{ser})) \tag{20}$$

The final form of equation (3-20) can be written as $S_{ser} = P_{ser} + jQ_{ser}$, where,

$$P_{ser} = rb_{ser}V_iV_j\sin(\delta_i - \delta_j + \theta_{ser}) - rb_{ser}V_i^2\sin\theta_{ser} \tag{21}$$

$$Q_{ser} = -rb_{ser}V_iV_j\cos(\delta_i - \delta_j + \theta_{ser}) + rb_{ser}V_i^2\cos\theta_{ser} + r^2b_{ser}V_i^2 \tag{22}$$

The reactive power delivered or absorbed by the shunt converter is independently controllable by the UPFC and can be modeled as a separate controllable shunt reactive source but it is not considered in this modeled. In this case the main function of reactive power is to maintain the voltage levels at bus i within acceptable limits. In view of the above explanations, Qshunt can be assumed to be 0[11]. Consequently, steady-state UPFC mathematical model is constructed from the series connected voltage source model with the addition of a power injection equivalent to P_{sh} + j0 to bus i, as shown in Fig.6.

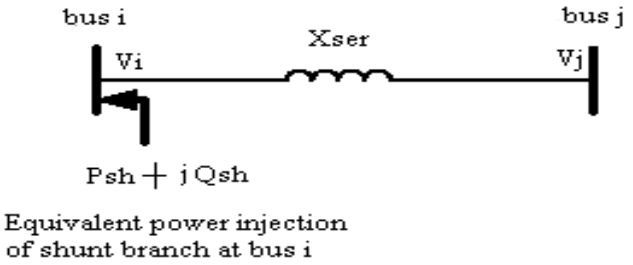

Figure (6): *Equivalent power injection of shunt branch*

4.3. Whole UPFC Injection Model:

Finally, steady-state UPFC mathematical model can be constructed by combining the series and shunt power injections at both bus i and bus j as shown in Fig.7.

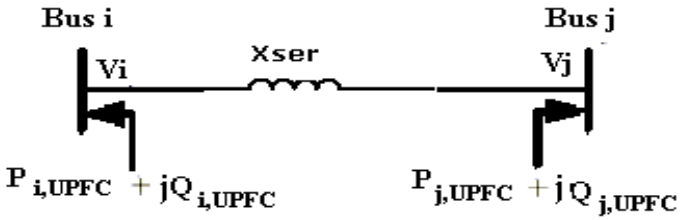

Figure (7): *Steady-state UPFC mathematical model*

Having $\delta_{ij} = \delta_i - \delta_j$, the elements of the equivalent power injections in Fig.7. are,

$P_{i,UPFC} = P_{iser} + P_{sh}$

$= 0.02\ r\ b_{ser}\ V_i^2 \sin\theta_{ser} - 1.02 r\ b_{ser}\ V_i\ V_j \sin(\delta_{ij}+\theta_{ser})$ (24)

$P_{j,UPFC} = P_{jser} = r b_{ser}\ V_i\ V_j \sin(\delta_{ij}+\theta_{ser})$ (25)

$Q_{i,UPFC} = Q_{iser} + Q_{sh} = -r\ b_{ser}\ V_i^2 \cos\theta_{ser}$ (26)

$Q_{j,UPFC} = Q_{jser} = r\ b_{ser}\ V_i\ V_j \cos(\delta_{ij}+\theta_{ser})$ (27)

5. Implementation:

For solving optimal power flow program the proposed algorithm is embedded with UPFC by using MATLAB. We referred to the program as *"unified power flow controller load flow"* (UPFCLF). Fig.3.6 describes the flow diagram of the programming process.

The general procedure of the proposed algorithm can be summarized as follows: the input system data includes the basic system data needed for conventional power flow calculation, *i.e.*, the number and types of buses, transmission line data, generation and load data, the location of UPFC, and the values of UPFC control parameters.

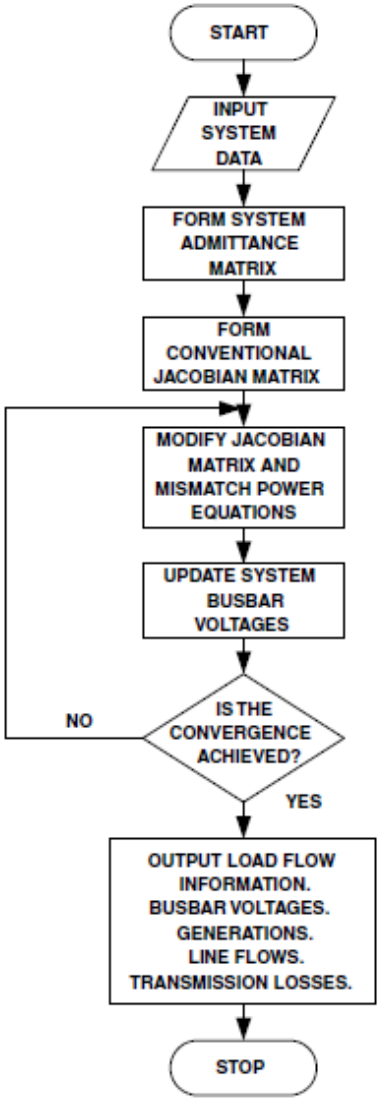

Figure(8):*Flow chart of the proposed power flow algorithm*

6. Case studies:

UPFC embedded power flow studies on IEEE 14-bus test system and IEEE 30-bus test system are carried out. It should be pointed out that the results are taken by the choice of UPFC parameters where r changes from 0.05 to 0.15 and θ_{ser} changes from 0° to 360°, i.e., the control parameters of UPFC (r, θ_{ser}) are given and UPFC is operated.

6.1. IEEE 14-bus test system:

6.1.1. Case (1):

14 bus system operates under condition of 100% of its original load with r=0.1 and different values of θ_{ser} which changes from 0° to 360°.

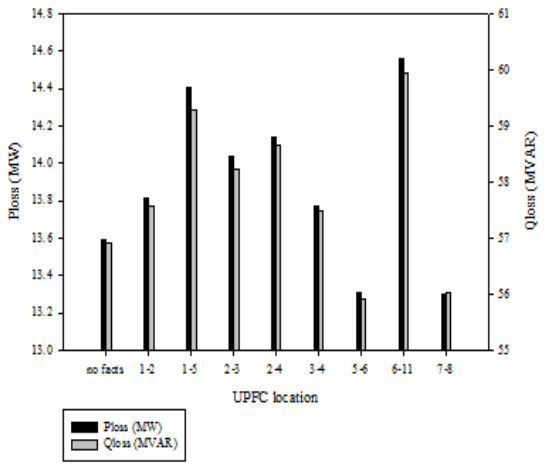

Figure (9): 14 bus system with UPFC parameters adjusted at r=0.1 and θ_{ser} =0°

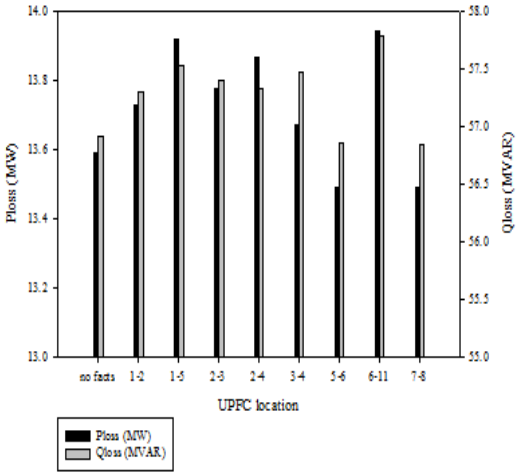

Figure (10): 14 bus system with UPFC parameters adjusted at r=0.1 and θ_{ser} =45°

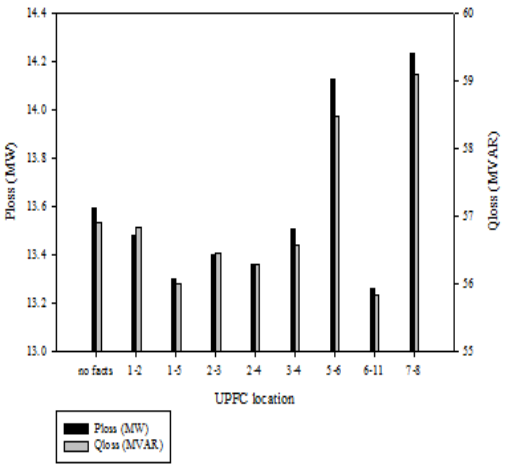

Figure (11): 14 bus system with UPFC parameters adjusted at r=0.1 and θ_{ser} =90°

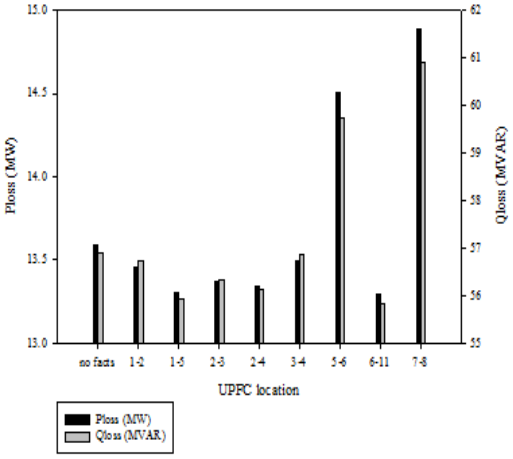

Figure (12): 14 bus system with UPFC parameters adjusted at r=0.1 and θ_{ser} =135°

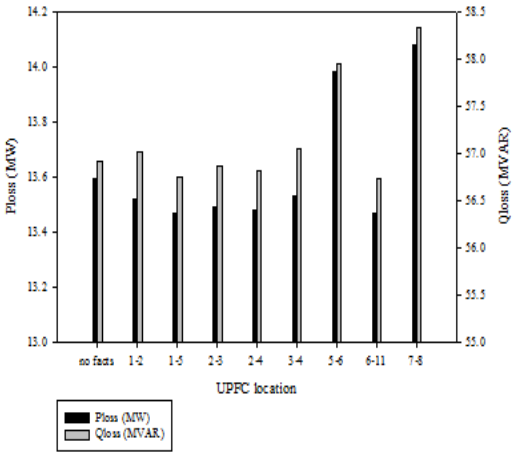

Figure (13): 14 bus system with UPFC parameters adjusted at r=0.1 and θ_{ser} =180°

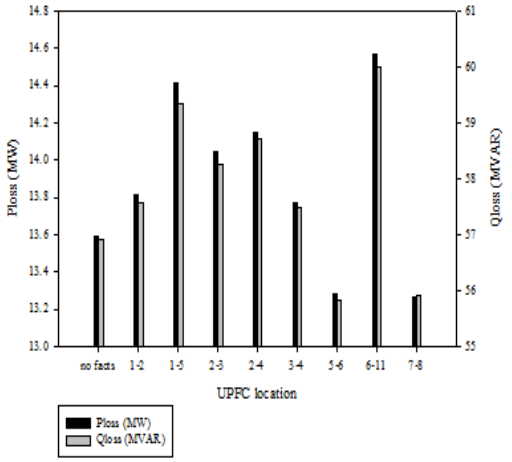

Figure (14): 14 bus system with UPFC parameters adjusted at r=0.1 and θ_{ser} =270°

As we see above by changing θ_{ser} values the active and reactive losses are affected. The least loss value is obtained at θ_{ser} =90° and UPFC is located between buses (6 and 11) and (6 and 12) and (6 and13). Also we get a quite similar result at θ_{ser} =270° and UPFC located between buses 7, 8.

Now we will explore the effect of changing the value of injected voltage r on line losses with θ_{ser} values 90° and 270°.

6.1.2. Case (2):

14 bus system operates under condition of 100% of its original load with r=0.05 and θ_{ser} =90°, 270°.

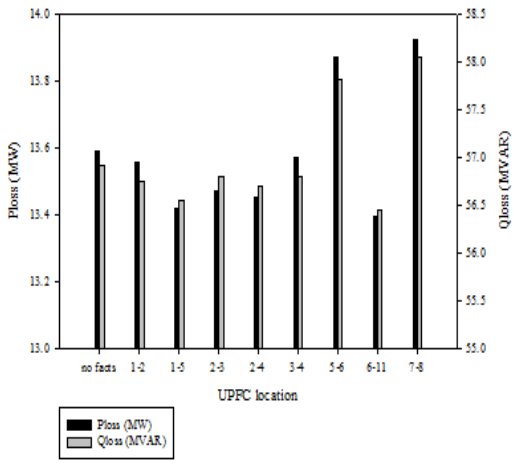

Fig. 15. 14 bus system with UPFC parameters adjusted at r=0.05 and θ_{ser} =90°

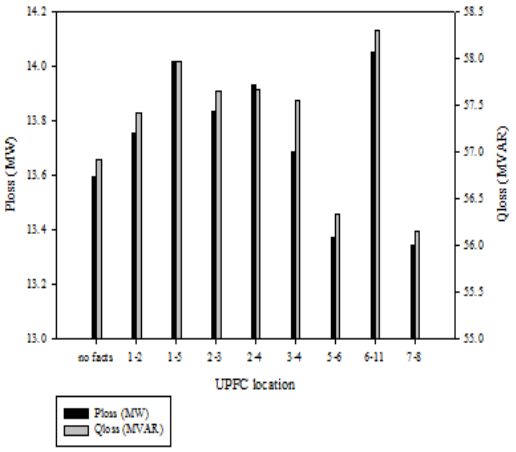

Fig. 16. 14 bus system with UPFC parameters adjusted at r=0.05 and θ_{ser} =270°

6.1.3. Case (3):

14 bus system operates under condition of 100% of its original load with r=0.15 and θ_{ser} =90°, 270°.

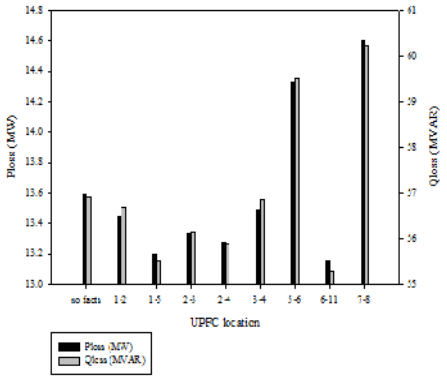

Fig. 17. 14 bus system with UPFC parameters adjusted at r=0.15 and θ_{ser} =90°

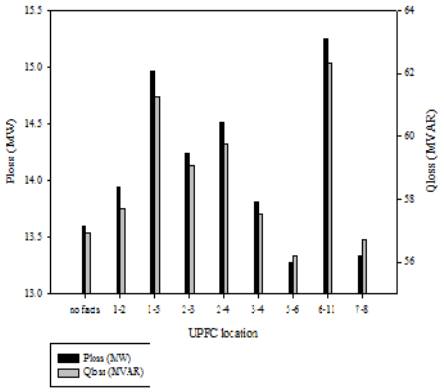

Fig. 18. 14 bus system with UPFC parameters adjusted at r=0.15 and θ_{ser} =270°

As we have mentioned the least active and reactive losses of the system are obtained for locating the UPFC at lines between buses (6and11), (6and12) and (6and13). For these three locations the best result is found to be with angle θ_{ser} =90°, but losses gradually increase with increasing θ_{ser} from 90° to 180°. As for the injected voltage magnitude effect, the higher value the lower the losses are, for example with r=0.15 we get less losses than when r=0.1. The losses decreases from 13.593 MW without UPFC to 13.151 MW with UPFC located near loads with adjusting its parameters at 0.15 p.u. and 90°.

6.2. IEEE 30-bus test system:

Different cases are studied on IEEE 30-bus test system with added-on UPFC are performed using UPFCLF. The electrical system is studied in order to determine the power flow in each of the transmission line without any compensation to have a general idea about system steady-state operation. Then UPFC is allocated on each line of the system and different UPFC parameters are set to activate UPFC, the transmitted active and reactive power of all of the lines has remarkably changed.
We will study IEEE 30-bus system for r =0.05, 0.1, 0.15 and θ_{ser} values 90° and 270°.

6.2.1. Case (1):

IEEE 30-bus system operates with its original load with different UPFC parameters.

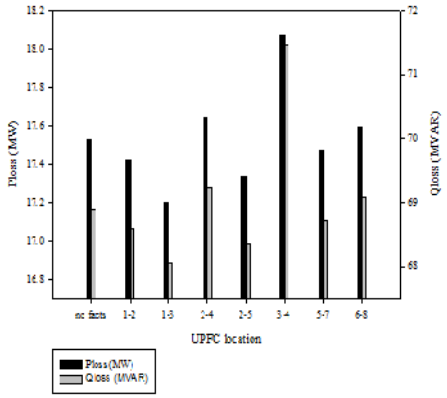

Fig. 19. 30 bus system with UPFC parameters adjusted at r=0.05 and θ_{ser} =90˚

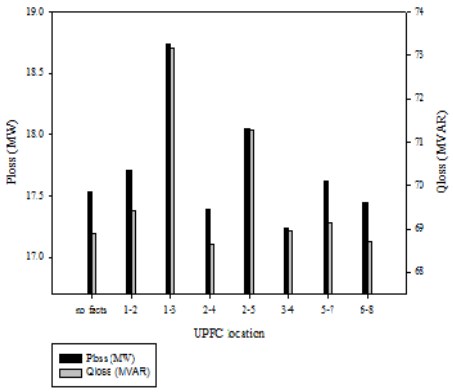

Fig. 20. 30 bus system with UPFC parameters adjusted at r=0.05 and θ_{ser} =270˚

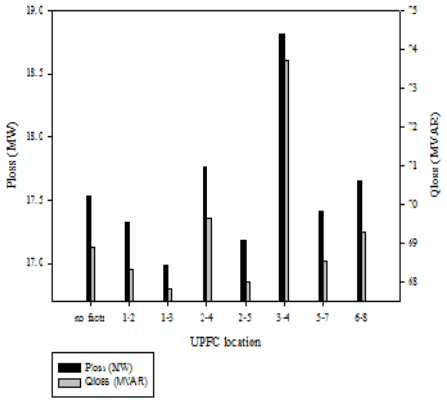

Fig. 21. 30 bus system with UPFC parameters adjusted at r=0.1 and θ_{ser} =90˚

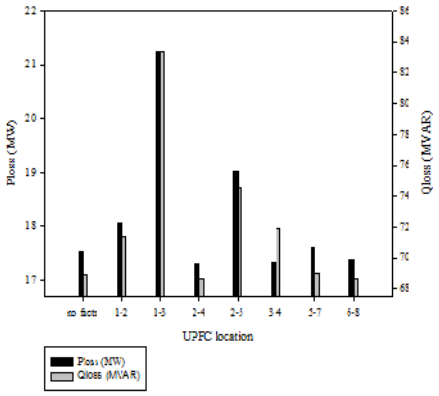

Fig. 22. 30 bus system with UPFC parameters adjusted at r=0.1 and θ_{ser} =270˚

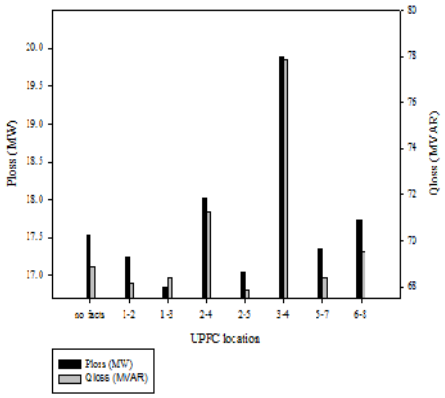

Fig. 23. 30 bus system with UPFC parameters adjusted at r=0.15 and θ_{ser} =90˚

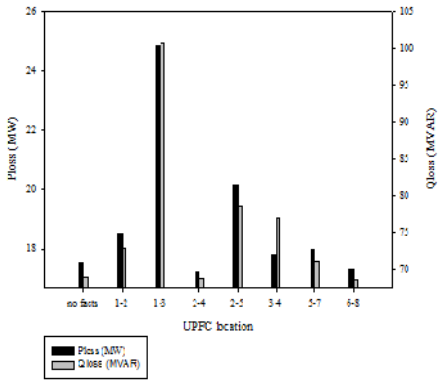

Fig. 24. 30 bus system with UPFC parameters adjusted at r=0.15 and θ_{ser} =270˚

Comparing power flow solutions of the system without and with locating UPFC between buses (1 and 3) shows the losses decreases from 17.528 MW to 16.98 MW and parameters of UPFC is adjusted at r=0.15 p.u. and θ_{ser} = 90°. It can be concluded that the proposed method developed in this study are efficient on analysis of both power flow and control parameters of UPFC.

From the previous results, it can be concluded that the system lines losses can be minimized by controlling the different control parameters (r, θ_{ser}) of UPFC. It can be noticed that UPFC location that gives least line losses appears in the generation zone, while locating it near loads will not affect power losses in the lines.

The observations we got indicate that for small systems, locating UPFC near loads zone provides better reduction of system line loss, while when in a network of large size we find an enhancement of the system line loss is obtained by locating the UPFC at generation zone.

6.3. Comparative graphical results of Effective of UPFC parameters on line loss:

During the simulation study, applied to the IEEE 14-bus system, it has been noted that the location of UPFC between busses 6 and 11, and varying UPFC parameters, r and θ_{ser} one at time, while keeping the second variable constant will lead to the results of the following figures.

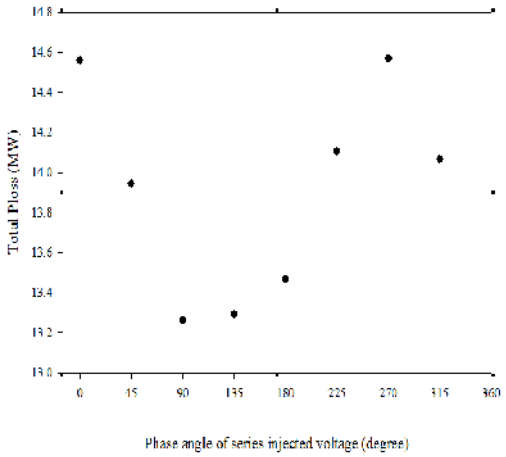

Fig. 25. Total active line losses via θ_{ser} and with r=0.1

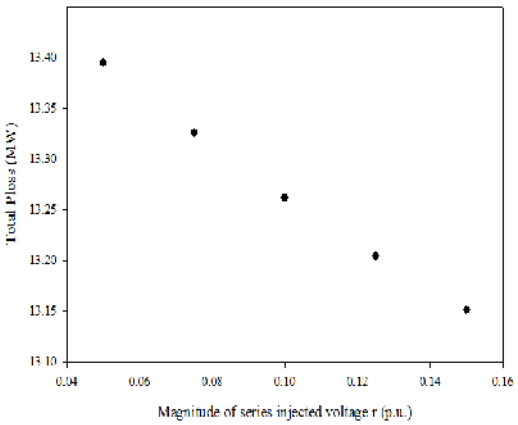

Fig. 26. Total active line losses via r and with θ_{ser} =90°

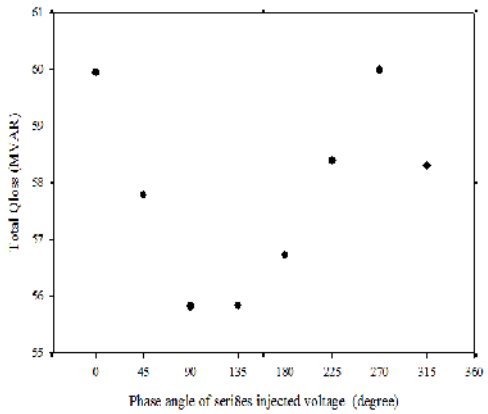

Fig. 27. Total reactive line losses via θ_{ser} and with r=0.1

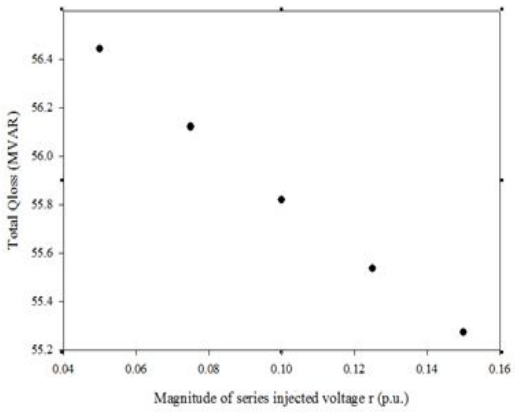

Fig. 28. Total reactive line losses via r and with θ_{ser} =90˚

These results show clearly that increasing parameter r leads to minimization of both active and reactive losses. The best results are found to take place when θ_{ser} =90.

7. Conclusion:

Insertion of UPFC model can be incorporated in optimal load flow program. The capability of UPFC control parameters in optimal power flow applications has been explained. It is clear that a UPFC can be controlled in a power system to satisfy the power system enhancement and minimization of the losses.

References:

[1] N.G.Higorani, "Flexible AC Transmission," IEEE Spectnim, P. 40-45, April 1993.

[2] M. Noroozian, L. Angquist, M. Ghandhari, G.Andersson. "Use of UPFC for optimal power flow control". IEEE Transactions on Power Delivery, Vol.12, No. 4, October 1997.

[3] Thomas John, " Line loss minimization and voltage regulation using UPFC" Elixir International Journal, Vol. 38, No. 2, pp. 4222-4224, 2011

[4] Y. Morioka, Y. Mishima and Y. Nakachi, Implementation of Unified Power Flow Controller and Verification for Transmission Capacity Improvement, IEEE Transactions on Power Systems, Vol. 14, No. 2, pp. 575-581, 1999.

[5] G.N. Taranto, L.M. Pinto and M.V. Pereira,Representation of FACTS Devices in Power System Economic Dispatch, IEEE Transaction on Power Systems, Vol. 7, pp. 572-576, May 1992.

[6] Fang Wanliang and Ngan H., A robust load flow technique for use in power systems with unified power flow controllers, Electric Power Systems Research ,Vol. 53,No.3,P.181–186,2000.

[7] A. Mete Vural and Mehmet Tu. ,Mathematical modeling and analysis of a unified power flow controller: A comparison of two approaches in power flow studies and effects of UPFC location, Electrical Power and Energy

Systems Vol. 29 ,P. 619–623,2007.

[8] Khaled Abdel-Aty Mohamed, Optimization of Power System Operation Using FACTS Devices, Electrical Power and Machines Department, Faculty of Engineering, Ain Shams University, pp. 11-31,2008..

[9] Noroozian M, Angquist L, Ghandhari M and Anderson G., Use of UPFC for optimal flow control. In: Stockholm power tech conference, Stockholm, Sweden, Vol.18, No. 22, P. 506–511 June1995.

[10] M. Noroozian, L. Angquist, M. Ghandhari and G. Andersson, Use of UPFC for Optimal Power Flow Control, IEEE Transaction on Power Delivery, Vol. 12, No. 4, P. 1629-1634, October 1997.

[11] Adit Pandita and Sanjay K. Jain, A Review on Power Flow Analysis with UPFC and its Applicability,International Journal of Engineering Research & Technology (IJERT), Vol. 2 ,No. 6, P. 2278-0181, June 2013.

[12] IEEE 14-bus test system data. Available from: <http://www.ee.washington.edu/research/pstca/pf14/pg_tca14bus.htm>.

[13] IEEE 30-bus test system data. Available from: <http://www.ee.washington.edu/research/pstca/pf30/pg_tca30bus.htm>.